Ind. Eng. Chem. Res. **1990**, *29*, 421-432.
Barnicki, S. D.; Fair, J. R. Separation System Synthesis: A Knowledge-Based Approach. 2. Gas/Vapor Mixtures. *Ind. Eng. Chem. Res.* **1992**, *31*, 1680-1694.
Barr, A.; Feigenbaum, E. *The Handbook of Artificial Intelligence*; Volume I; Addison-Wesley: Reading, MA, 1981.
Brunet, J. C. An Expert System for Solvent-Based Separation Process Synthesis. M.S. Thesis, Virginia Polytechnic Institute and State University, Blacksburg, VA, 1992.
ChemShare Corporation. *Design II User's Guide*; ChemShare Corporation: Houston, TX, 1985.
Cusack, R. W.; Fremeaux, P.; Glatz, D. A Fresh Look at Liquid-Liquid Extraction: Part I. Extraction Systems. *Chem. Eng.* **1991**, *98* (2), 66-76.
Douglas, J. M. *Conceptual Design of Chemical Process*; McGraw-Hill: New York, 1988.
Hanson, C. *Recent Developments in Liquid-Liquid Extraction*; Pergamon Press: Oxford, UK, 1971; p 117.
Henley, E. J.; Seader, J. D. *Equilibrium-Stage Separation Operations in Chemical Engineering*; Wiley: New York, 1981.
Keller, G. E. *Adsorption, Gas Absorption and Liquid-Liquid Extraction: Selecting a Process and Conserving Energy*; MIT Press: Cambridge, MA, 1982.
Kremser, A. Theoretical Analysis of Absorption Process. *Natl. Pet. News* **May 21, 1930**, *22* (*21*), 43-59.
Liu, Y. A.; Quantrille, T. E.; Cheng, S. H. Studies in Chemical Process Design and Synthesis. 9. A Unifying Method for the Synthesis of Multicomponent Separation Sequences with Sloppy Product Streams. *Ind. Eng. Chem. Res.* **1990**, *29*, 2227-2241.
Nelson, W. L. *Petroleum Refinery Engineering*; McGraw-Hill: New York, 1969; pp 850-858.
Nishida, N.; Stephanopoulos, G.; Westerberg, A. W. A Review of Process Synthesis. *AIChE J.* **1981**, *27*, 321-351.
Perry, R. H.; Green, D. *Perry's Chemical Engineers' Handbook*, 6th ed.; McGraw-Hill: New York, 1984.
Pratt, H. R. C. Computation of Stagewise and Differential Contactors: Plug Flow. In *Handbook of Solvent Extraction*; Lo, T. C., Baird, M. H. I., Hanson, C., Eds.; Wiley: New York, 1983; pp 151-198.
Quantrille, T. E.; Liu, Y. A. *Artificial Intelligence in Chemical Engineering*; Academic Press: San Deigo, CA, 1991.
Reissinger, K. H.; Schröter, J. Selection Criteria for Liquid-Liquid Extractors. *Chem. Eng.* **Nov 6, 1978**, *85* (11), 109-118.
Samdani, G. Editorial: Managing Knowledge. *Chem. Eng.* **1992a**, *99* (3), 5.
Samdani, G. Smart Software. *Chem. Eng.* **1992b**, *99* (3), 30-31 and 33.
Shaw, R. Editorial: Knowledge or Experience? *Chem. Eng.* (*Rugby, Engl.*) **March 12, 1992**, 3.
Sherwood, T. K.; Pigford, R. L. *Absorption and Extraction*, 2nd ed.; McGraw-Hill: New York, 1952; pp 211-214.
Simulation Sciences. *PROCESS (PRO II) Example Manual*; Simulation Sciences, Inc.: Fullerton, CA, 1987; p C5.
Smith, B. D. *Design of Equilibrium-Stage Processes*; McGraw-Hill: New York, 1963.
Treybal, R. E. *Mass-Transfer Operations*, 3rd ed.; McGraw-Hill: New York, 1980.
Wankat, P. C. *Separations in Chemical Engineering: Equilibrium-Staged Separations*; Elsevier: New York, 1988.
Wahnschaft, O. M.; Jarian, T. P.; Westerberg, A. W. SPLIT: A Separation Process Designer. *Comput. Chem. Eng.* **1991**, *15*, 565-581.

Received for review June 18, 1992
Revised manuscript received October 26, 1992
Accepted November 12, 1992

Nonlinear Model Predictive Control Using Second-Order Model Approximation

Sachin C. Patwardhan[†] and K. P. Madhavan*[,‡]
Systems and Control Group, Department of Electrical Engineering, and Department of Chemical Engineering, Indian Institute of Technology, Powai, Bombay 400 076, India

A model predictive control (MPC) algorithm using a nonlinear discrete perturbation model for lumped parameter systems has been proposed. The nonlinear ordinary differential equations (ODEs) representing the process are locally approximated using the terms up to second order in the Taylor expansion. Using regular perturbation technique and certain simplifying assumptions, the resulting equations are integrated over a sampling interval to obtain an approximate discrete model of the system. The Morse lemma is used to identify the conditions under which the proposed approximation will prove distinctly superior over the linear approximation. Under perfect model assumption, the performance of the proposed algorithm is demonstrated by simulating regulatory control of two continuously stirred tank reactors (CSTRs) characterized by zero steady-state gain with respect to one manipulated input at the optimum operating point and attendant change in the sign of the steady-state gain across the optimum. The MPC algorithm based on the proposed second-order model is shown to improve the closed loop performance when compared to other nonlinear MPC algorithms. Finally, it is shown that the proposed control algorithm is robust for moderate variations in plant parameters.

1. Introduction

The ever increasing quest for improvement in the performance of modern process plants and availability of fast computing power has given rise to the development of a new generation of advanced control algorithms which can identify the current optimal operating point of a process and effect the transition of the process to the new optimal point in an acceptable and safe manner. The resulting multivariable control problem with explicit constraint handling requirements has been successfully handled using model predictive control (MPC) techniques, such as dynamic matrix control (DMC) (Cutler and Ramaker, 1980) and model algorithmic control (MAC) (Richalet et al., 1978). However, these control algorithms, developed around linear prediction models, may not be adequate for handling strongly nonlinear systems often encountered in the process industry. With the need being recognized, a number of extensions of the MPC algorithms, which employ a nonlinear prediction model, have been recently proposed in the literature. On the basis of the approach

* To whom all correspondence should be addressed.
[†] Systems and Control Group, Department of Electrical Engineering.
[‡] Department of Chemical Engineering.

0888-5885/93/2632-0334$04.00/0

used to handle nonlinear ordinary differential equation (ODE) constraints representing the plant, these algorithms can be broadly classified into two categories, with methods employing locally linear approximations or the classical sensitivity equations for approximating local curvature falling in the first category and methods using orthogonal collocation technique for simultaneous solution and optimization in the second.

The orthogonal collocation method, which was originally suggested by Biegler (1984) for solving the optimal control problem, was extended by Patwardhan et al. (1990) to solve the nonlinear MPC problem with state variable constraints. The difficulties associated with the application of this method for a highly nonlinear system are selection of an appropriate polynomial approximation as a solution of the differential equations and increase in the dimension of the optimization problem with the increase in the number of collocation points.

Universal dynamic matrix control (UDMC) proposed by Morshedi (1986) as a nonlinear extension of the DMC algorithm requires the computationally demanding task of recomputing the "dynamic matrix" by integrating the nonlinear model and classical sensitivity equations at each optimization iteration. Economou and Morari (1986) advocated nonlinear internal model control (IMC) structure in which the inverse of the nonlinear model operator was obtained using successive substitution or a Newton type iterative procedure involving classical sensitivity equations. The limitation of Newton's method is that it is proposed as a single step and unconstrained control algorithm. The convergence problem of the Newton type control law was resolved by Li and Biegler (1988, 1989) through incorporation of a relaxation parameter (pseudo-Newton strategy). A single step, as well as multistep, control problem was posed as a quadratic programming (QP) problem with state and manipulated variable constraints. At every sampling instant, the multistep formulation requires computation of state derivatives along the prediction horizon by integrating sensitivity equations, thereby adding to the computational load. The relaxation parameter, which can be effectively used to ensure required damping, has to be calculated only iteratively at each sampling instant.

Brengel and Seider (1989) proposed an alternate multistep nonlinear predictive control algorithm using a linear perturbation model obtained at each sampling interval. Here the nonlinear model equations are linearized only at the beginning of the prediction horizon and used over the entire prediction horizon, thereby reducing the computational burden at the expense of prediction accuracy.

Though the methods based on linearization reduce computational load when compared to orthogonal collocation techniques, a linear approximation of the nonlinear model may not be admissible as a candidate to describe the local behavior in some specific situations involving highly nonlinear systems. One such pathological situation arises in the neighborhood of some points in the phase space where the sensitivity of output variable(s) with respect to one or more manipulated inputs reduces smoothly to zero (i.e., a zero local sensitivity situation is encountered). In situations such as these, there is motivation for looking at a better approximation of the nonlinear model equations.

This paper attempts to identify conditions under which linear approximation may be inadmissible in describing the local behavior of a nonlinear system and proceeds in evolving an alternate higher order approximation better suited for describing the local behavior in such cases. Using the proposed higher order model, a nonlinear model predictive control strategy is evolved and performance of the proposed algorithm is demonstrated by simulating regulatory control of two nonlinear processes.

2. Motivation for Using a Higher Order Perturbation Series Model

2.1. Theoretical Background. Consider a C^∞ nonlinear function f: $R^n \rightarrow R$ represented as $y = f(z)$. If the function "f" has a nonzero gradient at some $z_0 \in R^n$, then we can find a smooth change of coordinates, in some ball $\mathbf{U}(z_0,r) \subset R^n$ around z_0, by which the expression of function $f(z)$ on $\mathbf{U}$ becomes linear [$\delta_y = \nabla_z f|_{z_0}(z - z_0)$]. However, such locally linear change of coordinates is not possible if the function f has a *critical point* at $z = z_0$ [i.e., if $\nabla_z f|_{z_0} = \bar{0}$]. If $z = z_0$ is a *nondegenerate critical point* of function f, i.e., if the determinant of the Hessian of the function at the critical point is nonzero [$\det \nabla_{zz} f|_{z_0}) \neq 0$], then a basic result from topology known as the Morse lemma can be used to arrive at the coordinate transformation to describe the local behavior of $f(z)$ in the neighborhood of such a *nondegenerate* critical point. In general, such approximation will almost never be "numerically" exact, but there is a sense in which it is "geometrically" exact.

Morse Lemma (Poston and Stewart, 1977). Consider a C^∞ function f: $R^n \rightarrow R$ with a nondegenerate critical point at $z = z_0$. Then, in the neighborhood of the critical point, there is a smooth local change of coordinates to $y_1(z)$, $y_2(z)$, ..., $y_n(z)$ such that $y_1(z_0) = y_2(z_0) = \ldots = y_n(z_0) = 0$ and $f(z)$ takes an exact form

$$f(z_0) + \tfrac{1}{2}\sum_{i,j} \mathbf{H}_{ij}(z_0) y_i y_j \qquad (1)$$

Now, for smooth functions matrix $\mathbf{H}$ is symmetric, since $(\partial^2 f/\partial z_i\, \partial z_j = \partial^2 f/\partial z_j\, \partial z_i)$, and the following are obtained from linear algebra.

(i) There is a linear change of coordinates to

$$q_i = q_i(z_1, \ldots, z_n) \qquad i = 1, \ldots, n \qquad (2)$$

transforming eq 1 to the form

$$f(q) = f(0) - q_1^2 - q_2^2 - \ldots - q_s^2 + q_{s+1}^2 + \ldots + q_n^2 \qquad (3)$$

(ii) Though there are several ways of obtaining the form given by eq 3, they all have the same number (s) of negative terms and $n - s$ positive terms. The number s is called an "index" of the function $f(z)$ at $z = z_0$ and can be defined as the maximal dimension of a subspace of the vector space for which the Hessian is negative definite. The index of the resulting bilinear function on the vector space is a property of function f and is independent of the choice of coordinate system.

(iii) At the critical point, the function f will have a local minima if index $s = 0$, a local maxima if index $s = n$, or a saddle point if the index $0 < s < n$.

Definition. A C^∞ function f, $R^n \rightarrow R$, is called a Morse function if at every critical point the Hessian is nondegenerate.

Morse functions have the following nice properties.

Property 1. They are locally "simple", as they can be expressed everywhere either as linear functions in the neighborhood of a noncritical point or by a quadratic form as given by the Morse lemma.

Property 2. They are structurally stable. A small enough perturbation of a Morse function can always be expressed as the original function by a change of coordinates and of scale used for the values. So the local properties of a function f are shared by all perturbations of it.

2.2. Criteria for Selecting a Local Approximation. To understand the implications of the Morse lemma in the present context, consider the problem of obtaining a local

approximation for a general system represented by a nonlinear discrete model for piecewise constant inputs.

$$\mathbf{X}^{k+1} = \Xi(\mathbf{X}^k,\mathbf{U}^k) \tag{4}$$

$$\mathbf{Y}^{k+1} = \mathbf{C}\mathbf{X}^{k+1} \tag{5}$$

Here, $\Xi = \{\Xi_i\colon R^{n+m} \rightarrow R, i = 1, ..., n\}$ is a vector of nonlinear discrete functions. For the above functions, it may be argued that for a given fixed (or known) value of $\mathbf{X}^k$, the single step state and output predictions are functions of $\mathbf{U}^k$ alone. These functions (say $\xi_i\colon R^m \rightarrow R, i = 1, ..., n$) can be represented as

$$\mathbf{Y}^{k+1} = \mathbf{C}\xi(\mathbf{U}^k) = \mathbf{C}\xi(\mathbf{U}^{k-1} + \delta\mathbf{U}^k) \tag{6}$$

Now, the Morse lemma can be used to establish the order of approximation that can be used to represent the local behavior in the neighborhood of the point $(\mathbf{X}^k,\mathbf{U}^{k-1})$, as follows:

(i) A locally linear approximation for the ith output variable in the neighborhood of $\mathbf{U}^{k-1}$ can be used only if the ith row of the matrix $(\mathbf{C}\nabla_{\mathbf{U}}\xi)$ does not vanish at $\mathbf{U}^{k-1}$ (or $\mathbf{U}^{k-1}$ is a noncritical point of the ith output variable). The local linear approximation can then be written as

$$Y_i^{k+1} \simeq C_i(\xi(\mathbf{U}^{k-1}) + (\nabla_{\mathbf{U}}\xi)\ \delta\mathbf{U}^k) \tag{7}$$

where C_i is the ith row of matrix $\mathbf{C}$.

(ii) If the ith output (Y_i^{k+1}) has a critical point at some $\mathbf{U}^{k-1}$ and if the critical point is nondegenerate, then according to the Morse lemma the local behavior of the function in the neighborhood of this point is determined by the quadratic part of the Taylor expansion of the function. Thus, at the critical point, local approximation can be written as

$$Y_i^{k+1} = C_i[\xi_i(\mathbf{U}^{k-1}) + \omega^k] \tag{8}$$

where the ith element of the vector ω^k is given as

$$\omega^k(i) = \tfrac{1}{2}(\delta\mathbf{U}^k)^{\mathrm{T}}(\nabla_{\mathbf{UU}}\xi_i)\ \delta\mathbf{U}^k$$

if the following condition is satisfied

$$\det\left(\sum_j C_{ij}\nabla_{\mathbf{UU}}\xi_j\right) \neq 0$$

Here, C_i represents the ith row and C_{ij} represents the (i,j)th element of matrix $\mathbf{C}$.

Remark. In practice, it is unlikely that sensitivity of an output variable will vanish with respect to all the manipulated inputs. However, even if the sensitivity of the ith output variable with respect to one manipulated input (say the jth input, assuming the other independent inputs are held constant) vanishes smoothly at some isolated point, i.e.,

$$\left[\frac{\partial Y_i^{k+1}}{\partial U_j}\right]_{U_j = U_j^{k-1}} = 0 \tag{9}$$

then, a linear approximation may fail to describe local behavior of the ith output with respect to the jth manipulated input. In the neighborhood of such a point, the local behavior of the ith output with respect to the jth independent input can be expressed using second-order terms in a Taylor expansion provided the condition

$$\left(\frac{\partial^2 Y_i^{k+1}}{\partial (U_j)^2}\right)_{U_j = U_j^{k-1}} \neq 0 \tag{10}$$

is satisfied.

Though the above criteria may be used to arrive at a model structure that can approximate the local behavior of the discrete nonlinear system in the neighborhood of a given point, these criteria cannot be used to establish the "trust region" of the approximation. For approximating a highly nonlinear discrete system, the inclusion of second-order terms along with linear terms in the perturbation model can increase the trust region of the approximation in the neighborhood of noncritical points and generate a "geometrically exact" approximation in the neighborhood of the critical points. The second-order terms provide the change in sensitivity along the predicting trajectory thereby improving the prediction accuracy. The proposed model, which consists of linear and quadratic terms, retains the desirable features of the pseudo-Newton control algorithm (variable sensitivity along the prediction horizon) and the approach of Brengel and Seider (fixed point linearization at every sampling instant).

3. Control Algorithm Using the Second-Order Perturbation Model

In the NLMPC problem under consideration, it is required to minimize a square normed objective function involving future errors over a prediction horizon (P step prediction) by adjusting "M" future steps of manipulated input vectors subject to equality and inequality constraints. Thus, at the kth sampling instant ($t = t^k$), the control problem can be stated as

$$\min_{\mathbf{U}^k \ldots \mathbf{U}^{k+M-1}} \sum_{i=1}^{P} [(E^{k+i})^{\mathrm{T}}\mathbf{W}_{\mathbf{E}}(E^{k+i}) + (\Delta\mathbf{U}^{k+i})^{\mathrm{T}}\mathbf{W}_{\mathbf{U}}(\Delta\mathbf{U}^{k+i})] \tag{11}$$

where

$$\Delta\mathbf{U}^{k+i} = \mathbf{U}^{k+i} - \mathbf{U}^{k+i-1}$$

$$E^{k+i} = \mathbf{Y}_{\mathrm{r}} - \mathbf{Y}_{\mathrm{m}}^{k+i}$$

subject to

$$d\mathbf{X}_{\mathrm{m}}/dt = \mathbf{F}(\mathbf{X}_{\mathrm{m}},\mathbf{U}),\quad \mathbf{X}_{\mathrm{m}}(t^k) = \mathbf{X}_{\mathrm{m},0},\quad \text{and } \mathbf{U}(t^k) = U_0 \tag{12}$$

$$\mathbf{Y}_{\mathrm{m}} = \mathbf{C}\mathbf{X}_{\mathrm{m}} \tag{13}$$

$$\mathbf{H}(\mathbf{X}_{\mathrm{m}},\mathbf{U}) \leq \bar{0} \tag{14}$$

$$\mathbf{Q}(\mathbf{X}_{\mathrm{m}},\mathbf{U}) = \bar{0} \tag{15}$$

$$\Delta\mathbf{U}^{k+M} = \Delta\mathbf{U}^{k+M+1} = \ldots = \Delta\mathbf{U}^{k+P-1} = \bar{0} \tag{16}$$

$$\mathbf{U}^l \leq \mathbf{U}^{k+i} \leq \mathbf{U}^u \qquad i = 0, ..., M-1 \tag{17}$$

$$t \in [t^k, t^k + (P)T]$$

Here, vectors $\mathbf{X}_{\mathrm{m}}$ $(\in R^n)$ and $\mathbf{Y}_{\mathrm{m}}$ $(\in R^r)$ represent model state and output variables, respectively, vector $\mathbf{Y}_{\mathrm{r}}$ $(\in R^r)$ represents the set point vector, E^{k+i} represents the ith output prediction error, and the vector $\mathbf{U}$ $(\in R^m)$ represents the manipulated inputs. $\mathbf{W}_{\mathbf{E}}$ and $\mathbf{W}_{\mathbf{U}}$ are positive definite or positive semidefinite weighting matrices, and T denotes the sampling time.

3.1. Second-Order Perturbation Model. The main difficulty in obtaining the discrete perturbation models (such as eqs 7 and 8) is that the nonlinear functions ξ_i (or Ξ_i) may not be known exactly. However, approximate discrete perturbation models can be obtained from the system of nonlinear ODEs representing the process (eq 12) using the following two methods.

(1) Regular Perturbation Technique. The nonlinear ODEs are locally approximated using the terms up to second order in the Taylor expansion about the current operating point and the resulting equations are integrated over a sampling interval to obtain a discrete quadratic model.

(2) Solution of Sensitivity Equations. First- and second-order state derivatives follow certain differential equations (sensitivity equations) which can be integrated over the sampling interval to obtain a bilinear perturbation model. In the present study, only the regular perturbation approach has been presented.

The nonlinear function vector $\mathbf{F} = \{F_1, F_2, ..., F_n\}$ in eq 12 can be expanded as a multivariable Taylor series around the current operating point ($X_{m,0} = \mathbf{X}^k$, $U_0 = \mathbf{U}^{k-1}$), where k denotes the sampling instant, as

$$d\mathbf{X}_m/dt = \bar{\mathbf{F}}(\mathbf{X}_m^k,\mathbf{U}^{k-1}) + (\nabla_X\bar{\mathbf{F}})\Delta\mathbf{X}_m + (\nabla_U\bar{\mathbf{F}})\Delta\mathbf{U} + \tfrac{1}{2}\Delta\mathbf{X}_m^T(\nabla_{XX}\bar{\mathbf{F}})\Delta\mathbf{X}_m + \Delta\mathbf{X}_m^T(\nabla_{XU}\bar{\mathbf{F}})\Delta\mathbf{U} + \tfrac{1}{2}\Delta\mathbf{U}^T(\nabla_{UU}\bar{\mathbf{F}})\Delta\mathbf{U} + ... \quad (18)$$

where

$$\Delta\mathbf{X}_m = \mathbf{X}_m(t) - \mathbf{X}_m^k \quad \text{and} \quad \Delta\mathbf{U} = \mathbf{U}(t) - \mathbf{U}^{k-1}$$

Here, bar indicates that the corresponding derivatives are computed at the nominal state ($\mathbf{X}_m^k$,$\mathbf{U}^{k-1}$). Assuming that the input disturbances are small in some sense, the solution of eq 19 can be developed as an infinite series of terms representing first-order and higher order perturbation effects, as

$$\mathbf{X}_m = \mathbf{x}_{m,0} + \mathbf{x}_{m,1} + \mathbf{x}_{m,2} + ... \quad (19)$$

If the first term, $\mathbf{x}_{m,0}$, in the series is chosen as $\mathbf{X}_m^k$, then, by rearranging, we obtain

$$\mathbf{x}_m = \Delta\mathbf{X}_m = \mathbf{X}_m - \mathbf{X}_m^k = \mathbf{x}_{m,1} + \mathbf{x}_{m,2} + ... \quad (20)$$

Using regular perturbation technique (see Friedly (1973)), equations representing first- and second-order perturbation effects can be written as

$$d\mathbf{x}_{m,1}/dt = f^k + \mathbf{J}_X^k\mathbf{x}_{m,1} + \mathbf{J}_U^k\mathbf{u} \quad (21)$$

with the initial condition

$$\mathbf{x}_{m,1}(t^k) = 0 \quad (22)$$

and

$$d\mathbf{x}_{m,2}/dt = \mathbf{J}_X^k\mathbf{x}_{m,2} + \mathbf{Z}_1^k \quad (23)$$

with the initial condition

$$\mathbf{x}_{m,2}(t^k) = 0 \quad (24)$$

where

$$\mathbf{Z}_1^k(i) = \{\tfrac{1}{2}\mathbf{x}_{m,1}^T\mathbf{H}_{XX}^k(i)\mathbf{x}_{m,1} + \mathbf{x}_{m,1}^T\mathbf{H}_{XU}^k(i)\mathbf{u} + \tfrac{1}{2}\mathbf{u}^T\mathbf{H}_{UU}^k(i)\mathbf{u}\} \quad i = 1, ..., n$$

$$f^k = \bar{\mathbf{F}}(\mathbf{X}_m^k,\mathbf{U}^{k-1}), \quad \mathbf{J}_X^k = (\nabla_X\bar{\mathbf{F}}), \quad \mathbf{J}_U^k = (\nabla_U\bar{\mathbf{F}})$$

$$\mathbf{H}_{XX}^k(i) = \frac{\partial^2\bar{\mathbf{F}}_i}{\partial^2\mathbf{X}}, \quad \mathbf{H}_{XU}^k(i) = \frac{\partial^2\bar{\mathbf{F}}_i}{\partial\mathbf{X}\,\partial\mathbf{U}'}, \quad \mathbf{H}_{UU}^k(i) = \frac{\partial^2\bar{\mathbf{F}}_i}{\partial^2\mathbf{U}}$$

Here, $\mathbf{H}_{XX}^k(i)$, $\mathbf{H}_{XU}^k(i)$, and $\mathbf{H}_{UU}^k(i)$ are $(n \times n)$, $(n \times m)$, and $(m \times m)$ matrices, respectively for $i = 1, 2, ..., n$. Also, superscript k implies that the corresponding values of the derivatives are computed at kth control instant, i.e., at ($\mathbf{X}_m^k$,$\mathbf{U}^{k-1}$). Note that eq 23 is linear in $\mathbf{x}_{m,2}$ but has a nonhomogeneous term depending on the previous term $\mathbf{x}_{m,1}$ as well as the quadratic term in the deviation input ($\mathbf{u}^T\mathbf{H}_{UU}^k(i)\mathbf{u}$). An approximate discrete solution of these coupled differential equations can be obtained under certain simplifying assumptions listed below.

(i) The input vector $\mathbf{u}$ consists of a piecewise constant function represented as

$$\mathbf{u}(t) = \mathbf{u}^{k+j} \quad \text{for} \quad t^{k+j} < t \le t^{k+j+1} \quad j = 0, 1, 2, ..., P-1 \quad (25)$$

Here, $t^{k+j+1} = t^{k+j} + T$, where T is the sampling interval.

(ii) The equations for $\mathbf{x}_{m,1}$ and $\mathbf{x}_{m,2}$ are solved sequentially. While the equation for $\mathbf{x}_{m,2}$ is being solved, some average value of $\mathbf{x}_{m,1}$ over the sampling interval is used. Thus, for the ith prediction

$$\bar{\mathbf{x}}_{m,1}^{k+j} = (1-\lambda)\mathbf{x}_{m,1}^{k+j} + \lambda\mathbf{x}_{m,1}^{k+j+1} \quad (26)$$

where λ can take values

$\lambda = 0.5$ (average value approximation)

$\lambda = 1.0$ (terminal value approximation)

Under these assumptions, eqs 21 and 23 can be integrated over the prediction horizon to obtain a discrete prediction model, as

$$\mathbf{x}_{m,1}^{k+j+1} = \phi^k\mathbf{x}_{m,1}^{k+j} + \Gamma^k\mathbf{u}^{k+j} + \psi^k f^k \quad j = 0, ..., P-1 \quad (27)$$

with the initial condition

$$\mathbf{x}_{m,1}^k = \bar{0} \quad (28)$$

$$\mathbf{x}_{m,2}^{k+j+1} = \phi^k\mathbf{x}_{m,2}^{k+j} + \psi^k\zeta^{k+j} \quad j = 0, ..., P-1 \quad (29)$$

with the initial condition

$$\mathbf{x}_{m,2}^k = \bar{0} \quad (30)$$

where the ith element of vector ζ^{k+j} is given as

$$\zeta^{k+j}(i) = \{\tfrac{1}{2}(\bar{\mathbf{x}}_{m,1}^{k+j})^T\mathbf{H}_{XX}^k(i)(\bar{\mathbf{x}}_{m,1}^{k+j}) + (\bar{\mathbf{x}}_{m,1}^{k+j})^T\mathbf{H}_{XU}^k(i)(\mathbf{u}^{k+j}) + \tfrac{1}{2}(\mathbf{u}^{k+j})^T\mathbf{H}_{UU}^k(i)(\mathbf{u}^{k+j})\}, \quad i = 1, ..., n$$

and

$$\phi^k = \exp(\mathbf{J}_X^kT), \quad \Gamma^k = \int_0^T \exp(\mathbf{J}_X^k\tau)\mathbf{J}_U^k\,d\tau, \quad \text{and} \quad \psi^k = \int_0^T \exp(\mathbf{J}_X^k\tau)\,d\tau$$

The predicted future state variable trajectory is given by

$$\mathbf{x}_m^{k+j} = \mathbf{x}_{m,1}^{k+j} + \mathbf{x}_{m,2}^{k+j}, \quad j = 1, ..., P \quad (31)$$

$$\mathbf{X}_m^{k+j} = \mathbf{X}_m^k + \mathbf{x}_m^{k+j}, \quad j = 1, ..., P \quad (32)$$

while the output predictions can be written as

$$\mathbf{Y}_m^{k+j} = \mathbf{C}\mathbf{X}_m^{k+j}, \quad j = 1, ..., P \quad (33)$$

where $\mathbf{C}$ is a $(r \times n)$ output or observation matrix.

For single step prediction, using the initial conditions (28) and (30) with eq 32, it can be shown that the proposed second-order model closely approximates the required quadratic form, as

$$\mathbf{X}_m^{k+1} = \mathbf{X}_m^k + \psi^k f^k + \Gamma^k\mathbf{u}^k + \psi^k\eta^k \quad (34)$$

where the ith element of vector η^k ($i = 1, ..., n$) is given as

$$\eta^k(i) = \{\eta_0^k(i) + \eta_1^k(i)\mathbf{u}^k + (\mathbf{u}^k)^T\eta_2^k(i)\mathbf{u}^k\}$$

$$\eta_0^k(i) = \tfrac{1}{2}\lambda^2(\psi^kf^k)^T\mathbf{H}_{XX}^k(i)(\psi^kf^k)$$

$$\eta_1^k(i) = \lambda(\psi^kf^k)^T\{\lambda\mathbf{H}_{XX}^k(i)\Gamma^k + \mathbf{H}_{XU}^k(i)\}$$

$$\eta_2^k(i) = \{\tfrac{1}{2}\lambda^2(\Gamma^k)^T\mathbf{H}_{XX}^k(i)\Gamma^k + \lambda(\Gamma^k)^T\mathbf{H}_{XU}^k(i) + \tfrac{1}{2}\mathbf{H}_{UU}^k(i)\}$$

3.2. Correction for Unmeasured Disturbances and Model Mismatch. In general, it is not easy to evolve a simple and at the same time a rigorous correction strategy to account for the mismatch between the process response and the predicted model response for nonlinear systems. In the presence of a process–model mismatch, a rigorous approach could be re-identification of the nonlinear model

parameters; however, such approach is highly computation intensive. A simpler approach is to extend the disturbance correction strategy used in the case of linear MPC algorithms, where a linear correction term is used to compensate for the unmeasured disturbance and process-model mismatch. Thus, in the proposed algorithm the feedback is incorporated by correcting model prediction as

$$\mathbf{Y}_{mc}^{k+j} = \mathbf{Y}_{m}^{k+j} + d^{k} \quad j = 1, ..., P \tag{35}$$

and redefining the prediction error term in eq 11 as

$$E^{k+i} = \mathbf{Y}_{r} - \mathbf{Y}_{mc}^{k+i} \quad j = 1, ..., P \tag{36}$$

where the disturbance term d^k is estimated by finding the difference between the output measurement ($\mathbf{Y}^k$) and model prediction ($\mathbf{Y}_m^k$) at the kth sampling instant, as

$$d^{k} = \mathbf{Y}^{k} - \mathbf{Y}_{m}^{k} \tag{37}$$

The process-model mismatch can be reduced further, if the nonlinear model is used to account for the effect of previous control moves. Thus, the current model prediction ($\mathbf{Y}_m^k$) is computed by integrating the nonlinear model using a standard ODE solver instead of using the value obtained from the proposed approximate prediction model.

3.3. Control Algorithm. The steps involved in the control algorithm (at the kth sampling interval) can be summarized as follows: (i) measure the process output $\mathbf{Y}^k$, (ii) linearize the model at ($\mathbf{X}_m^k$,$\mathbf{U}^{k-1}$), (iii) initialize the future manipulated input profile to the profile obtained at the previous control interval, (iv) using the corrected prediction model, solve the optimization problem using any standard nonlinear optimization program to obtain the future input profile, (v) implement only the first move $\mathbf{U}^k = \mathbf{U}^{k-1} + \mathbf{u}^k$ on the process, (vi) integrate the model equations over one sampling interval using any standard nonlinear ODE solver to obtain $\mathbf{X}_m^{k+1}$ and $\mathbf{Y}_m^{k+1}$ by setting $\mathbf{U} = \mathbf{U}^k$, and (vii) set $k = k + 1$ and go to step i.

Analytical expressions for computing the sensitivity of the state variables with respect to the manipulated inputs are given in the Appendix. These sensitivity matrices can be used to obtain the analytical gradients of the performance objective and solve the optimization problem efficiently. Two versions of the nonlinear MPC algorithm can be considered: (1) the NLMPC1 algorithm (using locally linear prediction model) and (2) the NLMPC2 algorithm (using the proposed second-order prediction model). In the present study, the resulting nonlinear constrained optimization problem was solved using the *MATLAB Optimization Toolbox* routine "CONSTR" while MATLAB routine "ODE45" was used to integrate nonlinear model equations.

4. Simulation Examples

To demonstrate the effectiveness of the new algorithm, two regulatory control problems of continuously stirred tank reactors (CSTRs) were simulated. In the first example, regulatory control at the peak conversion of a CSTR with reversible reaction has been studied. This problem has been used by Li and Biegler (1988) to study the performance of single step pseudo-Newton control strategy. In the other simulation example, regulatory control of a continuous fermentor at the optimum operating point has been simulated. In both these reactors, the control problem is to maintain the operation at an extremum point where the process has zero steady-state gain with respect to one manipulated variable and the gain changes its sign across the extremum. Such a process under linear controller with integral action may produce an offset (Morari, 1983).

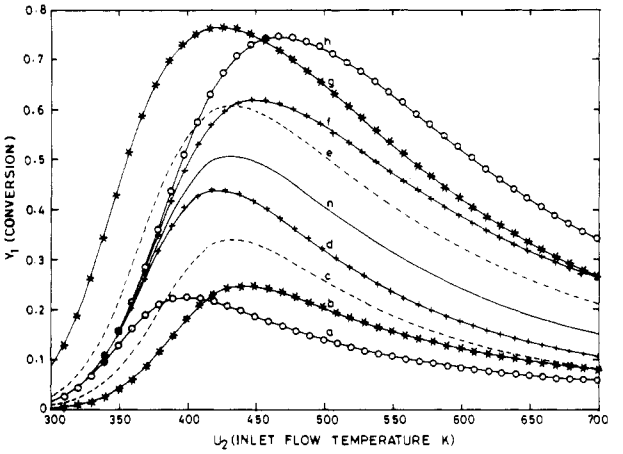

Figure 1. Example 1: reactor steady-state diagrams for nominal model and perturbations in kinetic parameters of plant. (n) nominal model, (a) $-10\%E_2$, (h) $+10\%E_2$, (b) $+10\%E_1$, (g) $-10\%E_1$, (c) $-50\%K_{0,1}$, (e) $+50\%K_{0,1}$, (d) $+50\%K_{0,2}$, (f) $-50\%K_{0,2}$.

In the sections that follow, the comparative simulation study of the NLMPC1 algorithm and NLMPC2 algorithm has been presented. In the case of the first reactor control problem, the results are also compared with a single step pseudo-Newton control algorithm (Li and Biegler, 1988).

4.1. Example 1. 4.1.1. Regulatory Control of CSTR. A first-order exothermic reversible reaction, represented as

$$\mathrm{A} \underset{K_2}{\overset{K_1}{\rightleftharpoons}} \mathrm{B} \tag{38}$$

is carried out in an ideal CSTR. It is assumed that the combined concentration of A and B remains constant during the reaction. Li and Biegler (1988) have presented the following dynamic model for the reactor

$$dX_1/dt = F_1(X,U) = -0.16X_1X_3^{-1}U_1 + K_1(1-X_1) - K_2X_1 \tag{39}$$

$$dX_2/dt = F_2(X,U) = 0.16U_1U_2X_3^{-1} - 0.16X_2X_3^{-1}U_1 + 5\{K_1(1-X_1) - K_2X_1\} \tag{40}$$

$$dX_3/dt = F_3(X,U) = 0.16U_1 - 0.4X_3^{0.5} \tag{41}$$

where

$$K_1 = K_{0,1}\exp(-E_1/X_2), \quad E_1 = 5000\ K, \quad \text{and} \quad K_{0,1} = 3 \times 10^5\ \text{min}^{-1}$$

$$K_2 = K_{0,2}\exp(-E_2/X_2), \quad E_2 = 7500\ \text{K}, \quad \text{and} \quad K_{0,2} = 6 \times 10^7\ \text{min}^{-1}$$

$$Y_1 = X_1 \quad \text{and} \quad Y_2 = X_3 \tag{42}$$

$$0 \le U_1 \le 2.5 \quad \text{and} \quad 300 \le U_2 \le 490.0 \tag{43}$$

Here, state variables X_1, X_2, and X_3 stand for conversion, reactor temperature, and liquid level in the reactor, respectively, and, the input variables U_1 and U_2 represent inlet flow and inlet flow temperature, respectively.

Analysis of the steady-state equations reveals that, for a fixed value of the inlet flow (and hence the level), the reactor equilibrium conversion as a function of inlet flow temperature has a well-defined maximum (see Figure 1, nominal model). The control problem is to move the conversion and level from the given initial condition to the maximum equilibrium conversion for the given level set point ($X_3 = 0.16$) by manipulating inlet flow and inlet flow temperature. The set point and the initial condition used

Table I

initial conditions	set points	initial conditions	set points
$X_1 = 0.16$	$Y_1 = 0.508779$	$X_3 = 0.12$ m	$Y_2 = 0.16$ m
$X_2 = 351.0$ K		$U_1 = 0.866$ L/min	
		$U_2 = 352.0$ K	

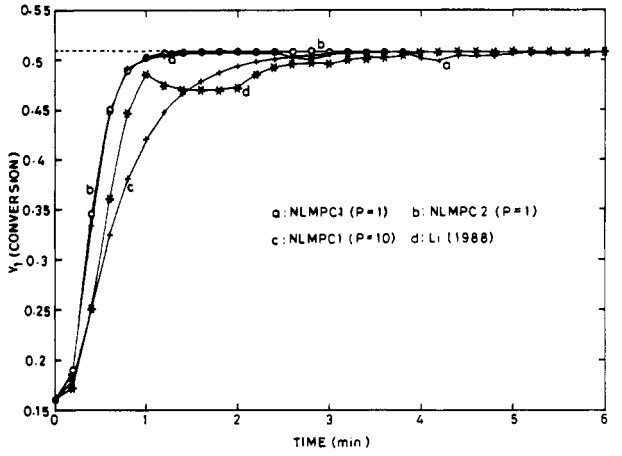

Figure 2. Example 1: Y_1 vs t (NLMPC1, NLMPC2, and results of Li (1988)).

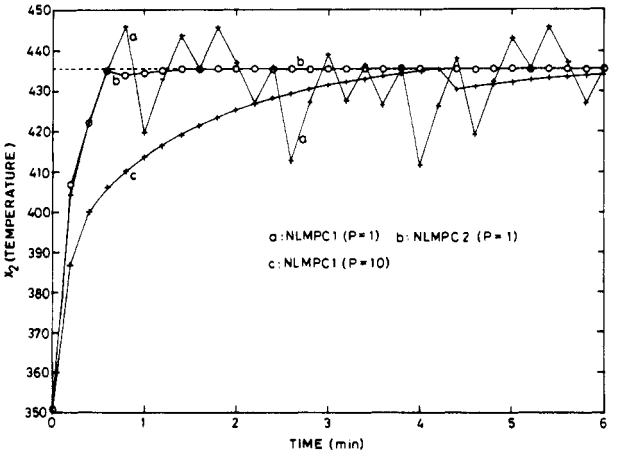

Figure 3. Example 1: X_2 vs t (NLMPC1 and NLMPC2).

in the simulation are given in Table I. The weighting matrix $\mathbf{W}_E$ is chosen as

$$\mathbf{W}_E = \text{diag}\,[10^6(1 \quad 100)] \tag{44}$$

while no weight is assigned on the control moves in the objective function. In order to improve the numerical stability of the optimizer, the input U_2 was scaled as $U_{2,sc} = U_2/100$ by appropriately modifying model equations.

The simulation results, under the perfect model assumption (i.e., there is no plant–model mismatch) are presented in Figures 2–6. When compared with the single step pseudo-Newton algorithm of Li and Biegler (1988), the single step NLMPC2 algorithm (with terminal value approximation) is seen to perform better in forcing the composition Y_1 and level Y_2 to reach their respective set points much faster along smoother trajectories than the pseudo-Newton controller. The variation in the inlet flow temperature (U_2) is also much less for the NLMPC2 algorithm. The superior performance of NLMPC2 can be attributed to the judicious choice of weights on errors in concentration and level in the objective function, a feature not exploited in the single step pseudo-Newton algorithm of Li and Biegler (1988).

The conversion trajectory (Y_1 vs time) is not significantly different when the single step NLMPC1 or NLMPC2 algorithm is used. The two single step algorithms show significant difference in the temperature response (X_2 vs time). While NLMPC2 is able to move the reactor temperature to the required steady value rapidly without overshoot or oscillation, the NLMPC1 algorithm produces an oscillatory temperature response. This oscillatory response in the uncontrolled state X_2 (temperature) is due to the large oscillations in U_2 (inlet flow temperature) resulting from the use of the single step NLMPC1 controller. The linear prediction model used in NLMPC1 cannot predict the change in the sign of the gain in the

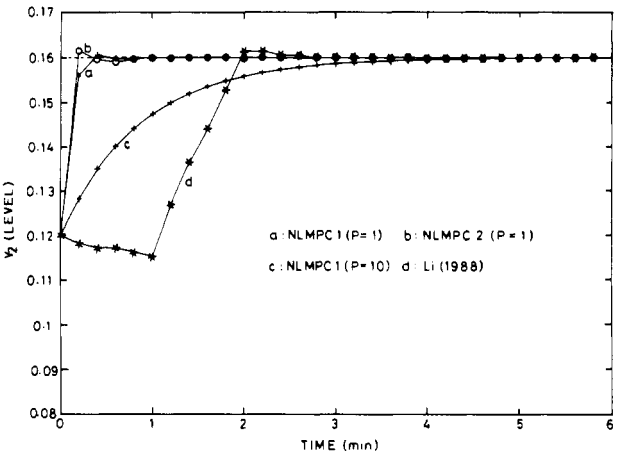

Figure 4. Example 1: Y_2 vs t (NLMPC1, NLMPC2, and results of Li (1988)).

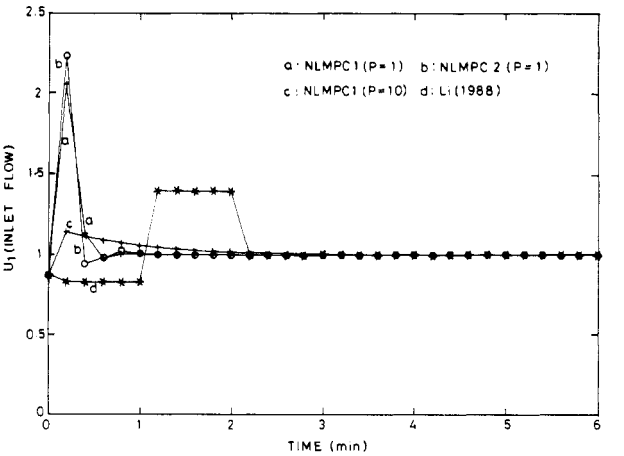

Figure 5. Example 1: U_1 vs t (NLMPC1, NLMPC2, and results of Li (1988)).

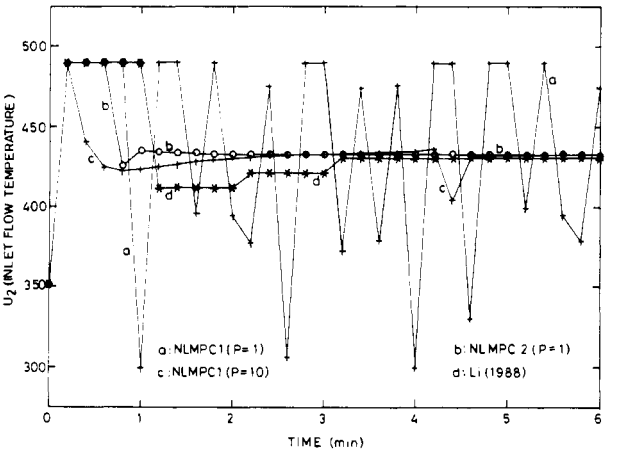

Figure 6. Example 1: U_2 vs t (NLMPC1, NLMPC2, and results of Li (1988)).

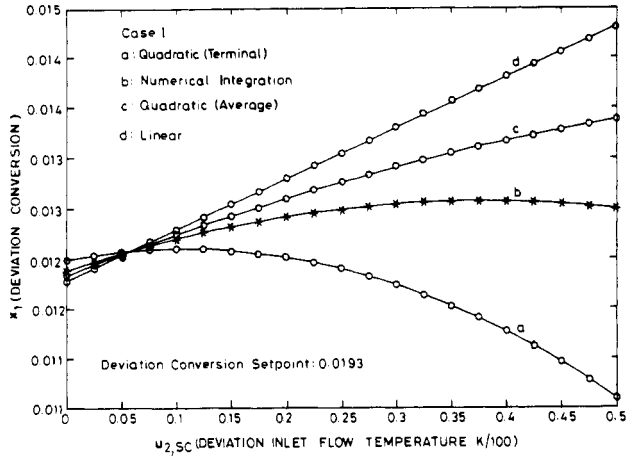

Figure 7. Example 1: Comparison of single step prediction models (case I).

neighborhood of the set point. Low values of sensitivity to inlet flow temperature in combination with the change in the sign of the gain across the peak conversion point gives rise to the oscillation in the inlet flow temperature when a single step algorithm is used.

In the case of the linear IMC algorithm, it has been shown that an increase in the horizon length (P) relative to the manipulated variable moves (M) plays a similar role as the input weighting matrix (Garcia and Morari, 1985). It is proposed that this strategy ($M = 1$ and relatively large P) be used to damp the oscillations in the manipulated input profile. A multistep NLMPC1 algorithm ($P = 10$, $M = 1$) is found to stabilize the temperature response. However this is realized at the expense of slower responses in Y_1.

To understand the difficulty associated with the control problem, consider the reduced model obtained by assuming the level and inlet flow to be constant ($X_3 = 0.16$ and $U_1 = 1.0$).

$$dX_1/dt = f_1(X_1,X_2,U_{2,sc}) = -X_1 + K_1(1 - X_1) - K_2X_1 \quad (45)$$

$$dX_2/dt = f_2(X_1,X_2,U_{2,sc}) = 100U_{2,sc} - X_2 + 5\{K_1(1 - X_1) - K_2X_1\} \quad (46)$$

From Figure 1, it may be observed that the optimum operating point is a critical point of the steady-state model. Also, if we differentiate the output Y_1 twice with respect to time, it can be observed that the zero sensitivity (of output with respect to manipulated input) situation can arise when the quantity

$$\frac{\partial f_1}{\partial X_2} = \frac{X_1E_2K_2 - (1 - X_1)E_1K_1}{(X_2)^2} \quad (47)$$

reduces to zero. In the neighborhood of such points a linear approximation of the nonlinear model will fail to describe the local behavior of the model. Consequently, near these points the controller (based on linear approximation) becomes ill conditioned and performs poorly unless safeguarded by constraints or by a suitable damping parameter (Biegler and Rawlings, 1991). Alternatively, the NLMPC2 controller based on the quadratic approximation of the discrete nonlinear model is shown to produce satisfactory performance at such a point without extreme variations in the manipulated input.

The relative performance of the NLMPC1 and NLMPC2 algorithm can be further analyzed by comparing the single step predictions of states obtained from the

Table II. Initial Condition I, NLMPC2 Controller ($300 \le U \le 490$)[a]

Case I: Sampling Instant (k) = 8

$$\mathbf{X}_m^k = [0.489\,528 \quad 433.966\,181 \quad 0.159\,642]^T$$

$$\mathbf{U}^{k-1} = [1.019\,101 \quad 425.5432]^T$$

first-order approximate

$$x_m^{k+1}(1) = 1.1787 \times 10^{-2} + 5.0603 \times 10^{-3}u_{2,sc}$$

second-order approximation (terminal)

$$x_m^{k+1}(1) = 1.2101 \times 10^{-2} - 9.7934 \times 10^{-3}(u_{2,sc} - u_2^*)^2$$

$$u_2^* = 0.1076$$

second-order approximation (average)

$$x_m^{k+1}(1) = 1.3741 \times 10^{-2} - 2.4484 \times 10^{-3}(u_{2,sc} - u_2^*)^2$$

$$u_2^* = 0.8817$$

Case II: Peak Conversion Point (Set Point)

first-order approximation

$$x_m^{k+1}(1) \cong 0$$

second-order approximation (terminal)

$$x_m^{k+1}(1) \cong -1.0051 \times 10^{-2}(u_{2,sc})^2$$

second-order approximation (average)

$$x_m^{k+1}(1) \cong -2.5127 \times 10^{-3}(u_{2,sc})^2$$

[a] Note: values smaller than 10^{-14} have been neglected.

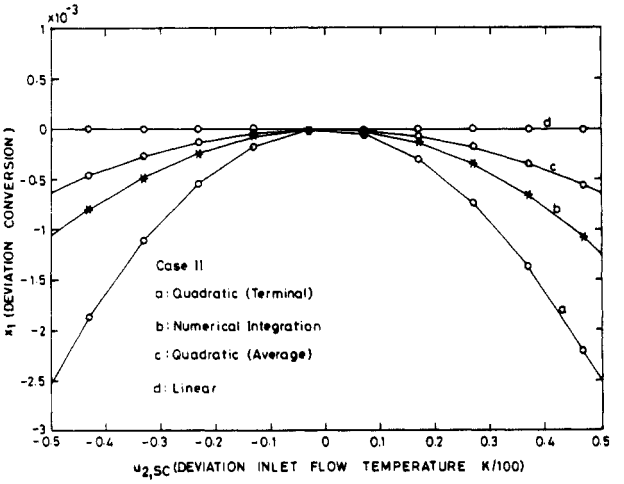

Figure 8. Example 1: Comparison of single step prediction models (case II).

respective first-order and second-order approximations with the single step predictions obtained by numerical integration of dynamic equations over one sampling interval (using ODE45 of MATLAB) for a given change in manipulated variable (deviation input $u_{2,sc}$). The analysis is done at two operating points, namely, a point close to the set point (case I) and a point at the set point (case II) which is an extremum (see Table II and Figures 7 and 8). From Table II and Figures 7 and 8, the following observations can be made.

(1) For case I, the linear model has a low sensitivity of x_1 with respect to input $u_{2,sc}$ and the control action $u_{2,sc}$ needed to move the predicted output to the set point will be large. For case II, the linear model is independent of $u_{2,sc}$ and the linear control law fails.

(2) Index of the proposed quadratic models in both cases is unity, indicating that, in both cases, the second-order

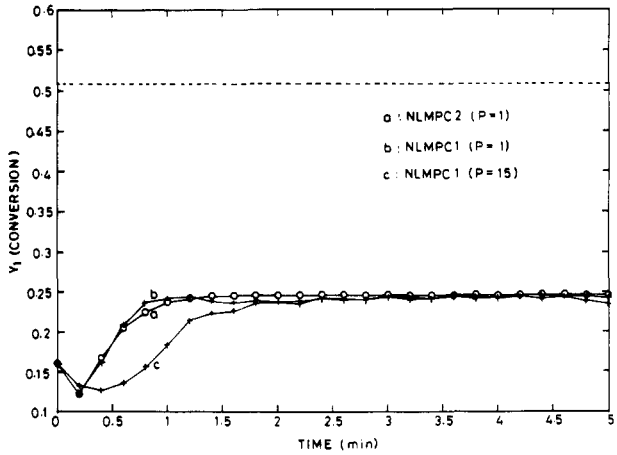

Figure 9. Example 1: Y_1 vs t (+10% perturbation in E_1).

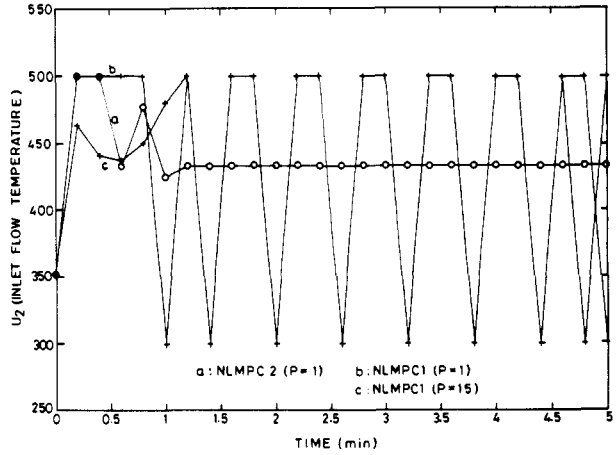

Figure 10. Example 1: U_2 vs t (+10% perturbation in E_1).

models will predict a maximum at their respective critical points. When compared to exact results from the numerical integration of the nonlinear model, it can be observed that, in both cases, single step predictions using the proposed second-order model are geometrically exact.

(3) From case I, it may be observed that when compared to the inlet flow temperature at the peak predicted using numerical integration ($u_{2,sc}$ = 0.37 or U_2 = 462.54 °C), the second-order model with average approximation overestimates the value of the inlet flow temperature at peak ($u_{2,sc}$ = 0.8817 or U_2 = 513.7 °C) while the second-order model with terminal approximation underestimates the inlet flow temperature at peak ($u_{2,sc}$ = 0.1076 or U_2 = 436.3 K). Thus, the second-order model with terminal value approximation is more robust as it predicts smaller variations in $u_{2,sc}$ to reach the maximum conversion in a single step from the neighborhood of the peak producing the damped inlet flow temperature profile.

(4) For case II, both versions of the second-order approximation models predict a peak at $u_{2,sc}$ = 0 (or U_2 = 433.08 °C). This is in agreement with the actual peak obtained by numerical integration.

4.1.2. Robustness against Model Mismatch. The specific nature of the reactor control problem studied in the earlier section, namely, control of the output variable at its extremum value, may pose robustness problems for the control algorithms like NLMPC1 or NLMPC2. To understand the nature of the control problem involved, the effect of perturbations in the kinetic parameters of the plant (±10% variations in E_1 and E_2, ±50% variations in $K_{0,1}$ and $K_{0,2}$) on the location of the steady-state maximum conversion has been studied, and the results are presented in Figure 1. From the simulation studies conducted to test robustness (with the input constraints, $0 \le U_1 \le 2.5$ and $300 \le U_2 \le 500$), the following general observations can be made on the robustness of the NLMPC1 and NLMPC2 algorithms (based on the nominal model).

(1) When the parameter perturbation shifts the maximum achievable conversion in the plant below the maximum conversion predicted by the nominal model, the conversion set point (based on the nominal model optimum) cannot be achieved, resulting in steady-state offset. Since the use of the mismatch correction term (d^k) has the effect of only shifting the origin of the linear and quadratic perturbation model while preserving their geometric characteristics, both NLMPC1 and NLMPC2 algorithms try to maximize conversion in the plant by moving toward the nominal model peak. The single step NLMPC2 algorithm maintains stable control with a non-oscillatory U_2 profile as the parabolic geometry of the quadratic approximation ensures the existence of a steady-state point for the plant at the minimum distance from the set point (see Figures 9 and 10). Both single step and multistep (P = 15, M = 1) NLMPC1 lead to oscillatory responses for U_2 due to low gain of the linear approximation in the neighborhood of the nominal model maximum, calling for large changes in U_2 to minimize the objective function. The oscillations do not get damped by extending the prediction horizon since there is a persistent offset in the conversion (Figures 9 and 10).

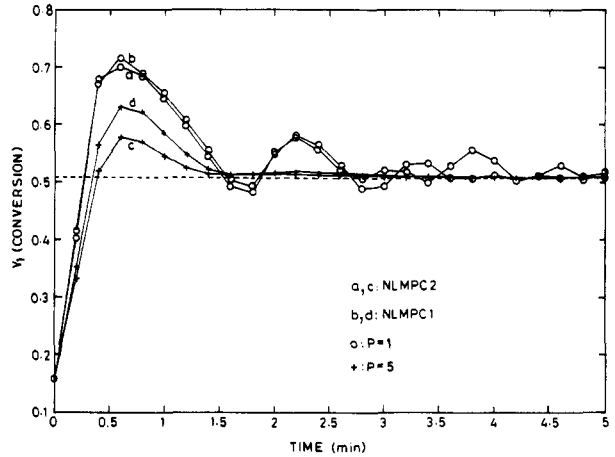

Figure 11. Example 1: Y_1 vs t (−10% perturbation in E_1).

(2) When the parameter perturbation shifts the maximum achievable conversion in the plant above the maximum conversion predicted by the nominal model, the conversion set point (based on the nominal model optimum) can be reached at an operating temperature away from the temperature at the nominal model peak (see Figure 1). In this region the nominal model has a dominant linear component which may influence the closed loop response. For example, in the case of −10% perturbation in E_1, the conversion set point can be reached at a temperature X_2 = 359.2 K (or U_2 = 357.6 K), as compared to the temperature at the nominal peak X_2 = 435.62 K (or U_2 = 433.08 K), and, at this operating temperature the steady-state gain of the nominal model is smaller than that of the corresponding steady-state plant gain (see Figure 1). Thus, both single step NLMPC1 and NLMPC2 algorithms give rise to oscillations in the U_2 response (see Figures 11 and 12). The use of multistep (P = 5, M = 1) NLMPC1 and NLMPC2 algorithms eliminates these oscillations.

4.2. Example 2. Control of Continuous Fermenters. Consider a well-mixed constant yield continuous fermenter,

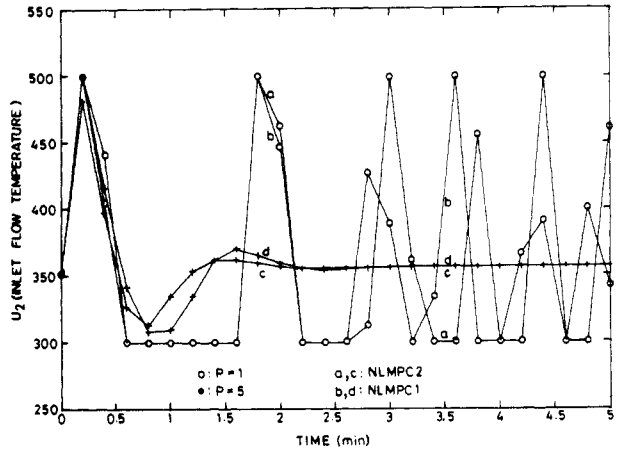

Figure 12. Example 1: U_2 vs t (−10% perturbation in E_1).

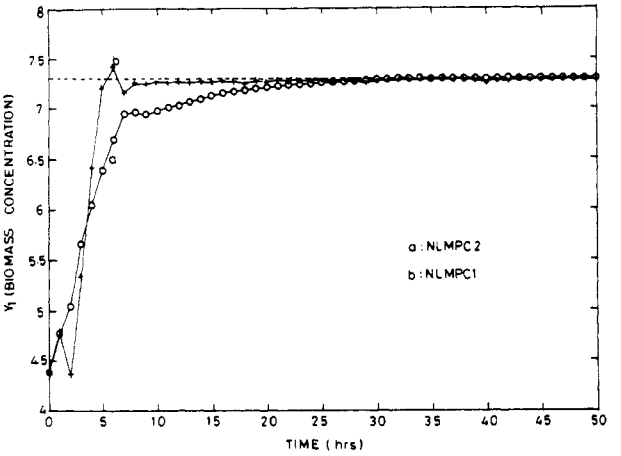

Figure 13. Example 2: Y_1 vs t (NLMPC1 and NLMPC2).

Table III

nominal model parameters	nominal model parameters
$Y_{X/S} = 0.4$ g/g	$P_m = 50$ g/L
$\alpha = 2.2$ g/g	$K_m = 1.2$ g/L
$\beta = 0.2$ h^{-1}	$K_i = 22$ g/L
$\mu_m = 0.48$ h^{-1}	

Table IV

initial conditions	optimum conditions	set points
$X_1 = 4.3866$ g/L	$X_1 = 7.3044$ g/L	$Y_1 = 7.3044$ g/L
$X_2 = 1.0335$ g/L	$X_2 = 5.138$ g/L	
$X_3 = 15.4993$ g/L	$X_3 = 24.9999$ g/L	$Y_2 = 24.9999$ g/L
$U_1 = 0.15$ h^{-1}	$U_1 = 0.1636$ h^{-1}	
$U_2 = 12.0$ g/L	$U_2 = 23.3991$ g/L	

with product free and sterile feed represented by the following unstructured model (Henson and Seborg, 1990)

$$dX_1/dt = F_1(X,U) = -U_1X_1 + \mu X_1 \quad (48)$$

$$\frac{dX_2}{dt} = F_2(X,U) = U_1(U_2 - X_2) - \frac{\mu X_1}{Y_{X/S}} \quad (49)$$

$$dX_3/dt = F_3(X,U) = -U_1X_3 + (\alpha\mu + \beta)X_1 \quad (50)$$

$$Y_1 = X_1 \text{ and } Y_2 = X_3$$

where the effluent biomass or the cell mass concentration (X_1), substrate concentration (X_2), and product concentration (X_3) are the process state variables and the dilution rate (U_1) and feed substrate concentration (U_2) are manipulated inputs. Using the substrate and product inhibition model, the specific growth rate (μ) is given as

$$\mu = \frac{\mu_m(1 - (X_3/P_m))X_2}{K_m + X_2 + (X_2^2/K_i)} \quad (51)$$

Also, $\alpha\mu + \beta$ is the specific product formation rate and $Y_{X/S}$ is the yield of cell mass with respect to the limiting substrate. The values of the different model parameters are given in Table III.

For most of the continuous fermentation processes the control objective is to maximize the productivity per unit time (productivity rate = U_1X_3). The optimum steady-state operating point can be obtain by maximizing the productivity rate using the dilution rate and feed substrate concentration as independent variables with steady-state model equations as constraints. The optimization results are presented in Table IV. The control objective is to move the system from the given initial condition to the optimum operating point.

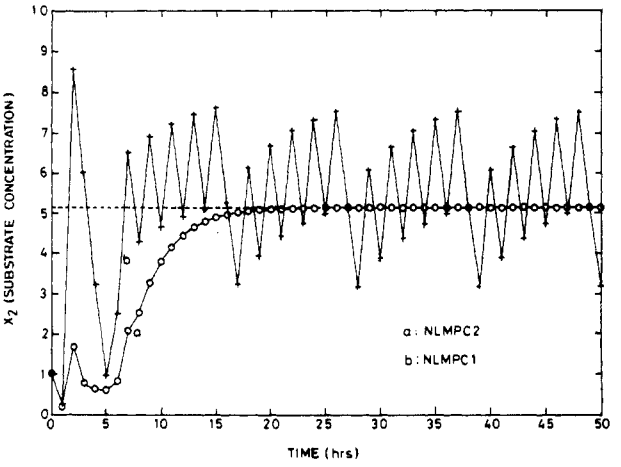

Figure 14. Example 2: X_2 vs t (NLMPC1 and NLMPC2).

The steady-state analysis reveals that, for constant U_1 ($U_1 = 0.1636$), the steady-state gains of Y_1 and Y_2 with respect to U_2 smoothly reduce to zero at the optimum operating point (or these are critical points of the steady-state equations for Y_1 and Y_2) and the sign of the gains changes across the optimum. Also, if we differentiate the outputs Y_1 and Y_2 twice with respect to time, a zero sensitivity to manipulated input situation can arise when the conditions

$$\partial F_1/\partial X_2 = X_1(\partial\mu/\partial X_2) = 0 \quad (52)$$

$$\partial F_3/\partial X_2 = \alpha X_1(\partial\mu/\partial X_2) = 0 \quad (53)$$

are satisfied.

The error weighting matrix in the objective function was chosen as

$$\mathbf{W}_E = \text{diag } [10^6(10 \quad 1)] \quad (54)$$

while the following constraints were imposed on the inputs

$$0 \le U_1 \le 0.25 \quad \text{and} \quad 10 \le U_2 \le 40 \quad (55)$$

Figures 13–17 compare the performance of the NLMPC1 algorithm with that of the NLMPC2 algorithm for perfect model assumption. It may be observed that the results obtained are qualitatively similar to those of the earlier example.

Conclusions

This paper has presented the development of an approximate second-order perturbation model which can be used for single step and multistep predictive control. The algorithm has been successfully implemented on two re-

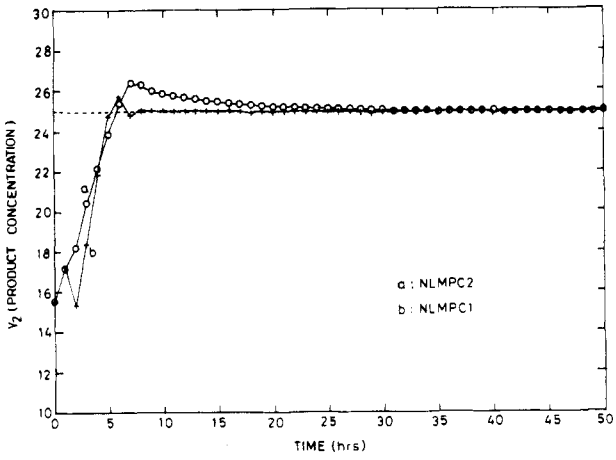

Figure 15. Example 2: Y_2 vs t (NLMPC1 and NLMPC2).

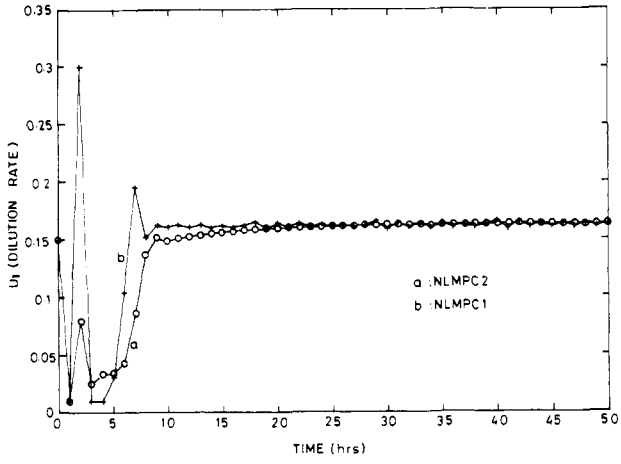

Figure 16. Example 2: U_1 vs t (NLMPC1 and NLMPC2).

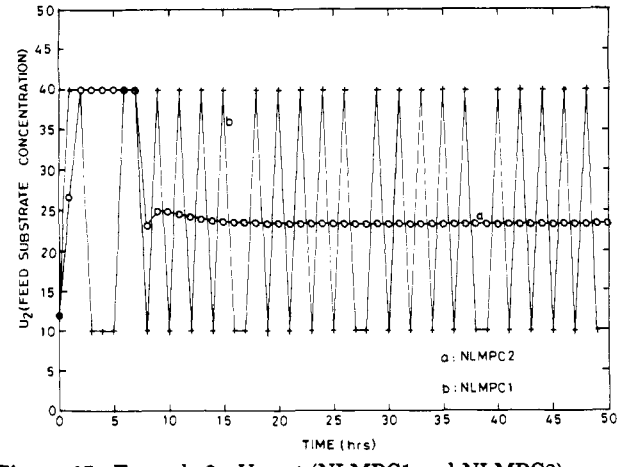

Figure 17. Example 2: U_2 vs t (NLMPC1 and NLMPC2).

actor control problems where the control objective is to operate the reactor at an extremum point. The control problem associated with the singular nature of the operating point has been successfully tackled by the proposed algorithm. The study has also provided some insight into the robustness issues of control at an extremum point through a classification of the robustness problems into two categories. The proposed algorithm has been found to be robust for moderate variations in the kinetic parameters.

Nomenclature

$\mathbf{C}$ = observation matrix
d = prediction correction
E = prediction error
E_i = kinetic parameters—example 1 (i = 1, 2)
$\mathbf{F}$ = function vector (see eq 12)
$\mathbf{H}_{XX}(i)$ = Hessian of ith element of vector $\mathbf{F}$ with respect to $\mathbf{X}$
$\mathbf{H}_{XU}(i)$ = Hessian of ith element of vector $\mathbf{F}$ with respect to $\mathbf{X}$ and $\mathbf{U}$
$\mathbf{H}_{UU}(i)$ = Hessian of ith element of vector $\mathbf{F}$ with respect to $\mathbf{U}$
$\mathbf{J}_X$ = Jacobian of vector $\mathbf{F}$ with respect to X
$\mathbf{J}_U$ = Jacobian of vector $\mathbf{F}$ with respect to U
$K_{0,i}$ = reaction constants—example 1 (i = 1, 2)
m = number of manipulated inputs
M = control horizon
n = number of state variables
P = prediction horizon
r = number of outputs
s = index of the Morse function
t = time
T = sampling interval
$\mathbf{U}$ = manipulated input vector
$\mathbf{u}$ = deviation manipulated input vector
$\mathbf{W}_E$ = error weighting matrices
$\mathbf{W}_U$ = input weighting matrices
$\mathbf{X}$ = state variable vector
$\mathbf{X}_m$ = model state variable vector
$\mathbf{x}_{m,i}$ = deviation model state variable vector (i = 1, 2)
$\mathbf{Y}$ = plant output vector
$\mathbf{Y}_m$ = model output vector
$\mathbf{Y}_{mc}$ = corrected model output vector
$\mathbf{Y}_r$ = set point vector

Greek Symbols

α = kinetic parameter—example 2
β = kinetic parameter—example 2
Γ = input sensitivity matrix
λ = parameter of eq 26
μ = specific growth rate—example 2
μ_m = maximum specific growth rate—example 2
η = parameter of eq 34
ϕ = state transition matrix
ψ = parameter of eqs 27–30
ω = parameter of eq 8
ξ = parameter of eq 6
Ξ = parameter of eq 4
ζ = second-order terms in proposed discrete perturbation model
$\mathbf{Z}$ = second-order terms in Taylor expansion of vector function $\mathbf{F}$

Superscripts

i = ith element/row/column
k = sampling instant k
$k + j$ = prediction of j instants ahead of instant k

Appendix: Analytical Derivatives of the Second-Order Model

It is possible to obtain an analytical expression to compute the sensitivity for the proposed second-order model. For example, for the case $M = P$, the sensitivity of the $(i+1)$th output prediction (i = 0, ..., P − 1) with respect to the jth future input (j = 0, ..., P − 1) can be written as

$$\left(\frac{\partial \mathbf{Y}_m^{k+i+1}}{\partial \mathbf{U}^{k+j}}\right) = \mathbf{C}\left(\frac{\partial \mathbf{x}_m^{k+i+1}}{\partial \mathbf{u}^{k+j}}\right) \tag{A1}$$

case $j < i$

$$\frac{\partial \mathbf{x}_m^{k+i+1}}{\partial \mathbf{u}^{k+j}} = \phi^k\left(\frac{\partial_m^{k+i}}{\partial \mathbf{u}^{k+j}}\right) + \psi^k\left(\frac{\partial \zeta^{k+i}}{\partial \mathbf{u}^{k+j}}\right) \tag{A2}$$

The lth row of the matrix $\partial \xi^k / \partial \mathbf{u}^k$ is given as

$$\left(\frac{\partial \zeta^{k+i}}{\partial \mathbf{u}^{k+j}}\right)_l = \{\mathbf{H}^k_{\mathbf{XX}}(i)(\bar{\mathbf{x}}^{k+i}_{\mathrm{m},l}) + \mathbf{H}^k_{\mathbf{XU}}(i)(\mathbf{u}^{k+j})\}^{\mathrm{T}}\left(\frac{\partial \bar{\mathbf{x}}^{k+j}_{\mathrm{m},l}}{\partial \mathbf{u}^{k+j}}\right)$$

where

$$\left(\frac{\partial \bar{\mathbf{x}}^{k+i}_{\mathrm{m},l}}{\partial \mathbf{u}^{k+j}}\right) = (1-\lambda)\left(\frac{\partial \bar{\mathbf{x}}^{k+i}_{\mathrm{m},l}}{\partial \mathbf{u}^{k+j}}\right) + \lambda\left(\frac{\partial \bar{\mathbf{x}}^{k+i+1}_{\mathrm{m},l}}{\partial \mathbf{u}^{k+j}}\right)$$

case $j = i$

$$\frac{\partial \mathbf{x}^{k+i+1}_{\mathrm{m}}}{\partial \mathbf{u}^{k+j}} = \Gamma^k + \psi^k\left(\frac{\partial \zeta^{k+i}}{\partial \mathbf{u}^{k+j}}\right) \tag{A3}$$

The lth row of the matrix $\partial \zeta^k / \partial \mathbf{u}^k$ is given as

$$\left(\frac{\partial \zeta^{k+i}}{\partial \mathbf{u}^{k+j}}\right)_l = \left[\left(\frac{\partial \bar{\mathbf{x}}^{k+i}_{\mathrm{m},l}}{\partial \mathbf{u}^{k+j}}\right)^{\mathrm{T}}\{\mathbf{H}^k_{\mathbf{XX}}(i)(\bar{\mathbf{x}}^{k+i}_{\mathrm{m},l}) + \mathbf{H}^k_{\mathbf{XU}}(i)(\mathbf{u}^{k+i})\} + (\mathbf{H}^k_{\mathbf{XU}}(i))^{\mathrm{T}}(\bar{\mathbf{x}}^{k+i}_{\mathrm{m},l}) + \mathbf{H}^k_{\mathbf{UU}}(i)(\mathbf{u}^{k+i})\right]^{\mathrm{T}}$$

where

$$\left(\frac{\partial \bar{\mathbf{x}}^{k+i}_{\mathrm{m},l}}{\partial \mathbf{u}^{k+j}}\right) = \lambda\left(\frac{\partial \mathbf{x}^{k+i}_{\mathrm{m},l}}{\partial \mathbf{u}^{k+j}}\right) = \lambda\Gamma^k$$

case $j > i$

$$\frac{\partial \mathbf{x}^{k+i+1}_{\mathrm{m}}}{\partial \mathbf{u}^{k+j}} = \bar{0} \tag{A4}$$

Literature Cited

Biegler, L. T. Solution of Dynamic Optimization Problems by Successive Quadratic Programming and Orthogonal Collocation. *Comput. Chem. Eng.* **1984**, *8* (3/4), 243–248.

Biegler, L. T.; Rawlings, J. B. Optimization Approaches to Nonlinear Model Predictive Control. In *Fourth International Conference on Chemical Process Control*, Padre Island, TX; Arkun, Y., Ray, W., H., Eds.; CACHE–AIChE: New York, 1991; pp 543–571.

Brengel, D. D.; Seider, W. D. Multistep Nonlinear Predictive Controller. *Ind. Eng. Chem. Res.* **1989**, *28*, 1812–1822.

Cutler, C. R.; Ramaker, B. L. Dynamic Matrix Control–A Computer Control Algorithm. *Proceedings of the Joint Automatic Control Conference*, San Francisco, CA; American Automatic Control Council: 1980.

Economou, C. G.; Morari, M. Internal Model Control. 5. Extension to Nonlinear Systems. *Ind. Eng. Chem. Process Des. Dev.* **1986**, *25*, 403.

Friedly, J. C. *Dynamic Behavior of Processes*; Prentice Hall: Englewood Cliffs, NJ, 1973; Chapter 3, pp 73–77.

Garcia, C. E.; Morari, M. Internal Model Control. 3. Multivariable Control Law Computation and Tuning Guidelines. *Ind. Eng. Chem. Process Des. Dev.* **1985**, *24*, 484–494.

Henson, M. A.; Seborg, D. E. Nonlinear Control Strategies for Continuous Fermenter. American Control Conference, San Diego, CA, 1990.

Li, W. C.; Biegler, L. T. Process Control Strategies for Constrained Nonlinear Systems. *Ind. Eng. Chem. Res.* **1988**, *27*, 1421–1433.

Li, W. C.; Biegler, L. T. Multistep, Newton Type Control Strategies for Constrained, Nonlinear Processes. *Chem. Eng. Res. Des.* **1989**, *67*, 562.

Morari, M. Robust Stability of Systems with Integral Control. *Proceedings of the Decision and Control Conference*, San Antonio, TX; IEEE Control Systems Society: 1983; p 865.

Morshedi, A. M. Universal Dynamic Matrix Control. In *Third International Conference on Chemical Process Control*; Morari, M., McAvoy, T. J., Eds.; CACHE Elsevier: New York, 1986.

Patwardhan, A. A.; Rawlings, J. B.; Edgar, T. F. Nonlinear Model Predictive Control. *Chem. Eng. Commun.* **1990**, *87*, 123–141.

Poston, T.; Stewart, I. N. A Sketch of Topologist's Calculus. In *Taylor Expansions and Catastrophes*; Research Notes in Mathematics 7; Pitman Publishing: London, 1977; pp 5–26.

Richalet, J. A.; Rault, A.; Testud, J. L.; Papon, J. Model Predictive Heuristic Control: Application To An Industrial Process. *Automatica* **1978**, *14*, 413–428.

Received for review May 7, 1992
Revised manuscript received September 9, 1992
Accepted October 5, 1992